Controls of Gradient Morphology and Surface Properties of Polymer Blends

Xu-Ming Xie,* Yue Chen, and Zeng-Min Zhang

Laboratory of Advanced Materials, Institute of Polymer Science and Engineering, Department of Chemical Engineering, Tsinghua University, Beijing 100084, Peoples Republic of China

Akihiko Tanioka

Department of Organic and Polymeric Materials, Tokyo Institute of Technology, 2-12-1, Ookayama, Meguro-Ku, Tokyo 152, Japan

Masami Matsuoka and Kenji Takemura

Kawasaki Plastics Laboratory, Showa Denko, Ltd., 3-2 Chidoricho, Kawasaki-Ku, Kawasaki 210, Japan

Received March 31, 1998; Revised Manuscript Received April 1, 1999

ABSTRACT: The phase morphology and surface composition of ethylene−vinyl acetate (EVAc) and polypropylene (PP) blends were investigated in this work. It was found that the 70/30 PP/EVAc blend formed a gradient phase morphology in the cross section by annealing. The particle size of the EVAc dispersed phase increased gradually along the direction vertical to the sample surface from the middle to the surface with increasing annealing time and temperature. The EVAc component on the surface of the blends after annealing was detected using Fourier transform infrared spectroscopy coupled with attenuated total reflectance (ATR-FTIR) and electron spectroscopy for chemical analysis (ESCA). The oxygen consistent with the EVAc on the surface of the PP/EVAc blends (70/30) also increases with increasing time and temperature. It means that the component of the EVAc accumulates on the surface with the formation of the gradient phase morphology in the blends. No significant difference in the gradient phase morphology was found for both the thin and thick PP/EVAc blend samples at the same annealing conditions. Moreover, the EVAc copolymer was melt-grafted with acrylamide (AAm) and then blended with PP. It was also found that PP/EVAc-*g*-AAm formed a gradient phase structure during annealing, the same as that of a PP/EVAc blend. With the dispersed phase EVAc as a carrier, the grafted polar groups were transported onto the surface of the blend sample with formation of an EVAc gradient dispersed phase. Thus, the gradient phase structure control of blends is an effective method for the material surface modification of materials.

Introduction

The surface composition and concentration of polymers influence many of their properties and applications, such as wetting, coating, adhesion, dyeing, friction, and biocompatibility. In particular, for general polymers, with their nonpolarity, applications have been restricted. At present, many chemical and physical methods have been used to modify the surface properties of polymer materials. Most of these methods introduce polar functional groups directly onto the surface. On the other hand, it has long been recognized that the surface composition of a multicomponent polymer system is usually different from the bulk[1−5] and that the surface segregation of one component in the polymer blends can be expected. The blending or mixing of polymers is an inexpensive route to the modification of various polymer properties. Due to its utility and simplicity, blending is currently attracting more attention as a feasible method for improving polymer surface properties.[5−8]

Hitherto, many studies on surface modification through the blending or mixing of polymers have been predominantly reported concerning the effect of surface selectivity at the surface/polymer interface.[9−14] This effect is believed to relate to the polymer surface region that is only several or several tens of angstroms thick.

In our previous papers,[5,15,16] it was found that PP/EVAc blends could take the form of unique gradient dispersed phase structures in vertical sections by annealing. The particle size of the dispersed phase EVAc gradually increased along the direction to the sample surface from the center to the surface. It was also shown that the EVAc component in the blends increased along the vertical direction of the sample from the center to the surface with the formation of a gradient morphology. These results provide us the possibility of modifying the surface properties of polymers and of obtaining the desired polymer blend performance through the control of the phase morphology.

In this study, we present the gradient phase morphology of the PP/EVAc 70/30 blend as a function of annealing time and temperature by using scanning electron microscopy (SEM). The surface composition of the blends was detected by using ATR-FTIR and ESCA. The relation between the formation of the gradient phase morphology and the component accumulation on the surface of the blends is also discussed. Furthermore, EVAc was melt-grafted with AAm and then blended with PP. It is expected that through heat treatment the modified dispersed phase can form the gradient morphology in the PP matrix. With EVAc as a carrier, the grafted polar groups were transported onto the surface of the material while forming an EVAc gradient dispersed phase.

* To whom correspondence should be addressed.

10.1021/ma9805046 CCC: $18.00
Published on Web 06/10/1999

Experimental Section

Materials. The PP resin used in this study was a homopolymer, having a melt flow rate of 7.2 g/10 min ($M_w = 25 \times 10^4$), made by Showa Denko Co. The EVAcs were random copolymers containing 33 wt % vinyl acetate, having a melt flow rate of 31 g/10 min, and were made by Mitsui-Du Pont Chemicals Co. The AAm monomers and BPO used were commercially available with analytical grade.

Melt-Grafting Reaction and Characterization of the Melt-Grafted EVAc-*g*-AAm. The melt-grafting reaction of AAm on EVAc was carried out using a Brabender. Benzoyl peroxide (BPO) was used as the initiator, and the temperature was 100 °C. The reaction was done in a dry nitrogen atmosphere. The resulting compounds were first dissolved in diethyl ether. Some deionized water was then added to remove the PAAm. The remaining samples were EVAc and EVAc-*g*-AAm. Then the sample thus obtained was pressed into a piece of thin film and analyzed by FTIR. FTIR spectra were recorded on a Nicolet 20SXC spectrometer. Two hundred scans at a resolution of 4 cm^{-1} were used to obtain spectra from samples. The optimum conditions were obtained through studying the effects of temperature and different amounts of monomer and initiator on the grafting. These optimum conditions included a temperature of 100 °C, the VAc = 100phr, the AAm = 10phr, and the initiator BPO at 0.2phr.

Preparation of Blends. A 70/30 blend of PP and EVAc was compounded on a Brabender Plasti-Corder equipped with a 50 cm^3 sample chamber at 170 °C, with a rotor speed of 35 rpm. The torque was 350 N m. The components were first dry blended. About 5 min of mixing time was required for complete dispersion of the blend. The torque was continuously recorded during the mixing. Sheets used in the measurement were prepared by the following procedure. The appropriate blend samples were placed a mold and laminated between two pieces of polyimide (PI) or polytetrafluorethylene (PTFE) film and then melt-pressed after preheating for 10 min to mold a sheet at various temperatures and annealed as a function of time. After annealing, the molding was rapidly quenched in ice water. The molded sheets were about 1 and 2 mm thick.

The blends of the melt-grafted EVAc and PP were prepared into a 1 mm thick sheet the same as the PP/EVAc blends.

SEM Observation. The phase morphologies of the molded sheets were examined using scanning electron microscopy (SEM). The sections were obtained using a Reichert-Nissei Ultracut N type ultramicrotome under a liquid-nitrogen atmosphere. These sections were then stained by exposure to the vapors of an aqueous solution of 0.5% ruthenium tetraoxide (RuO_4) for 4 h to enhance the contrast between the phases and subsequently carbon-plated by evaporation, using a JEOL JEE-3X vaccum evaporator. All observations were carried out on a JEOL JSM-T3330A SEM.

For the PP/EVAc-*g*-HEMA blend sheets, the cross sections were obtained with the microtome. The sections were then etched by using hexane or diethyl ether and observed under the SEM.

ATR-FTIR Measurement. ATR-FTIR spectra were recorded on a Nicolet 20SXC spectrometer outfitted with a variable-angle Harrick DRA-2C2 ATR attachment. The internal reflection elements chosen were 45° KRS-5. Two hundred scans at a resolution of 4 cm^{-1} were used to obtain spectra from samples pressed against KRS-5 under a dry nitrogen purge.

ESCA Measurement. ESCA analysis was performed on a SSX-100 spectrometer (Surface Science Instruments, Mountain View, CA) using a monochromatic Al K X-ray source and a detection system with a 35° solid angle acceptance lens, a hemispherical analyzer, and a position-sensitive detector. The standard operating conditions of the X-ray source were 10 kV and 12 mA. The base pressure of the instrument was 2×10^{-9} Torr and an operating pressure of 2×10^{-8} Torr. Survey scans (0−1000 eV BE) were run at an analyzer pass energy of 150 eV and an X-ray spot size of 600 μm to determine the elemental composition of each blend. High-resolution O 1s and Cl 1s spectra were obtained at a pass energy of 25 eV. All data analysis was carried out using a Hewlett-Packard computer analyzer.

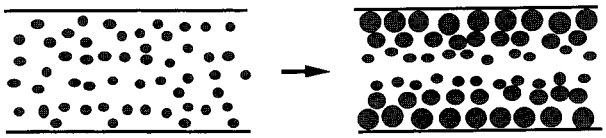

Figure 1. Schematic diagram of the formation of the gradient phase morphology.

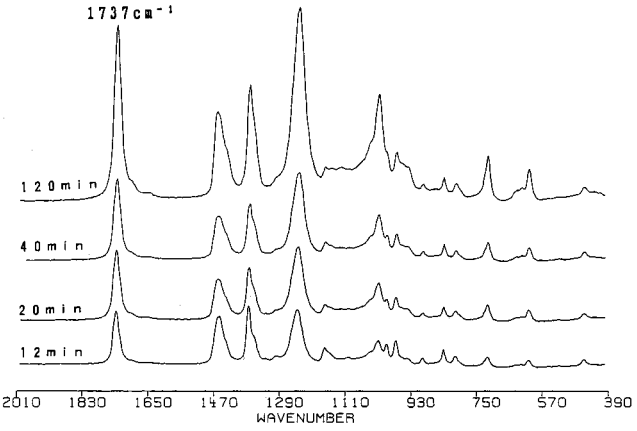

Figure 2. ATR-FTIR spectrum on the surface of the 70/30 PP/EVAc blends at 220 °C for various annealing times.

Examination of Coating Adhesion Test. Blend surfaces were tested by the following procedure: Without primer, the PP/EVAc-*g*-AAm blend sample surface was first etched by hexane and coated with polyurethane (PU) paints and then put into an oven at 120 °C to dry for 12 h. The coating on the blend samples was then cut into 10 mm strips. The peeling strength of the coating was measured by using an ASTM D903 180° peel test.

Results and Discussion

Figure 1 shows the scheme of the initial dispersed phase EVAc with the uniform distribution in the PP matrix to form the gradient phase morphology during annealing. This was reported in our previous paper.[5] For a short annealing time, the EVAc particles of the dispersed phase in the PP matrix have a small size and are distributed uniformly. When the annealing time is longer, the particle size increased in the vicinity of the sample surface, and the gradient morphology of the dispersed phase has been formed. The longer the annealing time, the more the particle size of the dispersed phase grew from the inside to the surface. An image analysis has shown that the EVAc concentration in the vicinity of the surface is higher than that in the bulk for the blend sample that formed the gradient phase morphology.[5]

To examine how the surface composition changes with changing phase morphologies in the blends, the surface composition of the blend was detected using an ATR-FTIR spectrometer. Figure 2 shows the spectra of the sample surface of the blends for various annealing times. It is observed that the intensity of the band at 1737 cm^{-1} for EVAc increases with increasing annealing times. The absorbance band at 1737 cm^{-1} in the spectra is assignable to the carbonyl stretching vibration of EVAc. Also, the absorbance band at 1454 cm^{-1} can be assigned as being caused by the vibration of the methylene group of PP. This means that the EVAc component accumulated on the surface of the blend with the

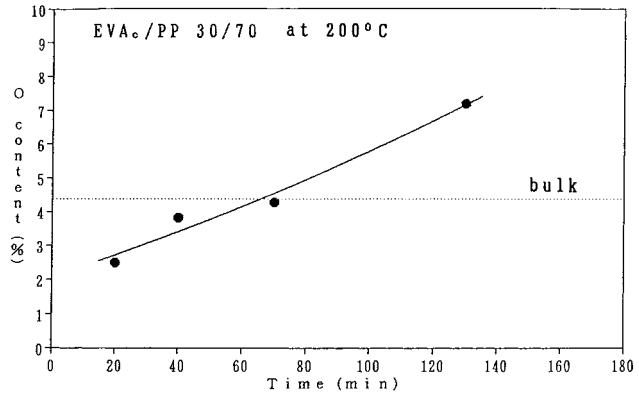

Figure 3. Plot of oxygen content on the surface of PP/EVAc blends versus the annealing times.

formation of the gradient phase morphology, and the more the gradient phase morphology formed, the more the EVAc component enriched the sample surface.

However, ESCA is another spectroscopic tool that provides sufficient surface sensitivity for a polymer film. In contrast to the depth of analysis of a few micrometers for ATR-FTIR, it is only several angstroms for ESCA; i.e., the information on a thin layer at the sample's surface of the blends can be obtained using ESCA. In fact, ESCA measurements used as a quantitative method to analyze the elemental composition of the surface of polymers is well established. Because the only atoms present in our samples were carbon and oxygen, and oxygen only exists in EVAc, to detect the ratio of the elemental composition of sample's surface, we can easily obtain the concentration of the EVAc component on the surface of the blends. The results of the ESCA experiments are plotted against the annealing times of the blends shown in Figure 3. The oxygen content on the sample surface of the blends increases with increasing annealing times. This result is the same as that of ATR-FTIR and suggests surface enrichment in polymer blends by controlling the dispersed phase morphology as a gradient.

The changes in the morphology in the cross section of the 70/30 PP/EVAc blend sample with a 1 mm thickness were also observed when changing the annealing temperature for a fixed time of 70 min.[15] At the lower temperature, no obvious gradient morphology of the EVAc dispersed phase was formed in the PP matrix. When the annealing temperature is higher, the EVAc gradient phase morphology was formed, and the higher the annealing temperature, the greater the gradient phase morphology is formed. The spectra of the sample surface of the blends are shown in Figure 4 for the various annealing temperatures. It is obvious that the intensity of the 1737 cm^{-1} band for the EVAc component on the blend surface increased with increasing annealing temperatures, corresponding to the formation of the gradient phase morphology. The oxygen content on the sample surface of the blends is plotted versus the annealing temperature in Figure 5. The oxygen content at the sample surface increased with increasing annealing temperatures and is much greater than that of the bulk at the higher temperatures.

The dependence of the formation rate of the gradient phase morphology on the annealing temperature and time indicates that the coalescence of the dispersed phase plays an important role in the gradient phase morphology.[17,18] The formation of the large particles of

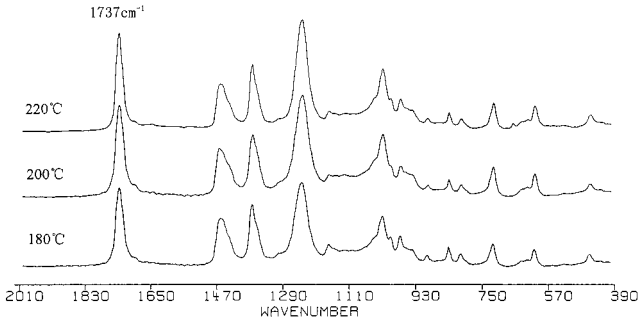

Figure 4. ATR-FTIR spectrum on the surface of the 70/30 PP/EVAc blends anealed for 70 min at various annealing temperatures.

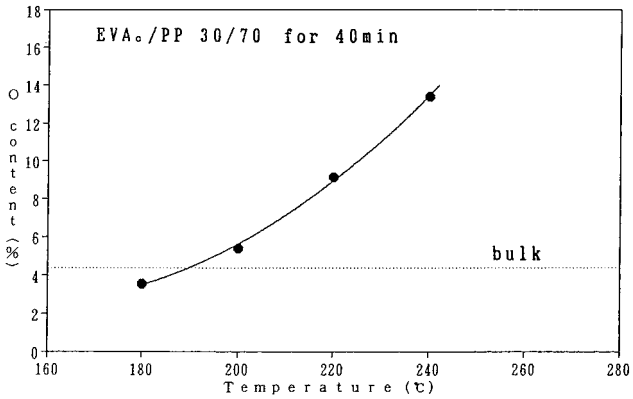

Figure 5. Plot of oxygen content on the surface of PP/EVAc blends versus the annealing temperature.

the dispersed phase in the vicinity of the sample surface leads to an increase in the concentration and accumulation on the sample surface of the EVAc component.

Figure 6 shows the SEM micrographs of the cross section of the 70/30 PP/EVAc blends of 2 and 1 mm thicknesses annealed for 70 min at 220 °C. For the thicker blend sample, the gradient phase morphology formed like that of the thinner sample. It should be noted that the EVAc particle sizes in the vicinity of the blend sample surface are almost the same, and the thickness of about 250 μm of the gradient morphology region is also almost the same for both the 2 and 1 mm thick samples. This indicates that there is no significant difference in the formation rate of the gradient phase morphology for both the thin and thick samples with the same annealing conditions.

The ATR-FTIR spectra of the sample surface for the blend of different thicknesses are shown in Figure 7. It was observed that the intensity of the 1737 cm^{-1} band for the 1 mm thick sample is slightly stronger than that of the 2 mm thick blend; i.e., the concentration of the dispersed phase accumulated on the surface corresponds to the formation of the gradient phase morphology.

Moreover, it is well-known that the properties of the multicomponent polymer system on the surface are dramatically affected by the surface (interfacial) energy and, therefore, are different from the properties in bulk. We prepared the blend samples laminated between polyimide (PI) and polytetrafluorethylene (PTFE) films and annealed at 220 °C for 70 min. Despite the different contact substrates, no definite difference was observed in the EVAc dispersed phase morphologies of the two sides of the sample in the cross section. We discussed the cause and the growth mechanism of the gradient phase morphology of polymer blends in another papers.[17,18]

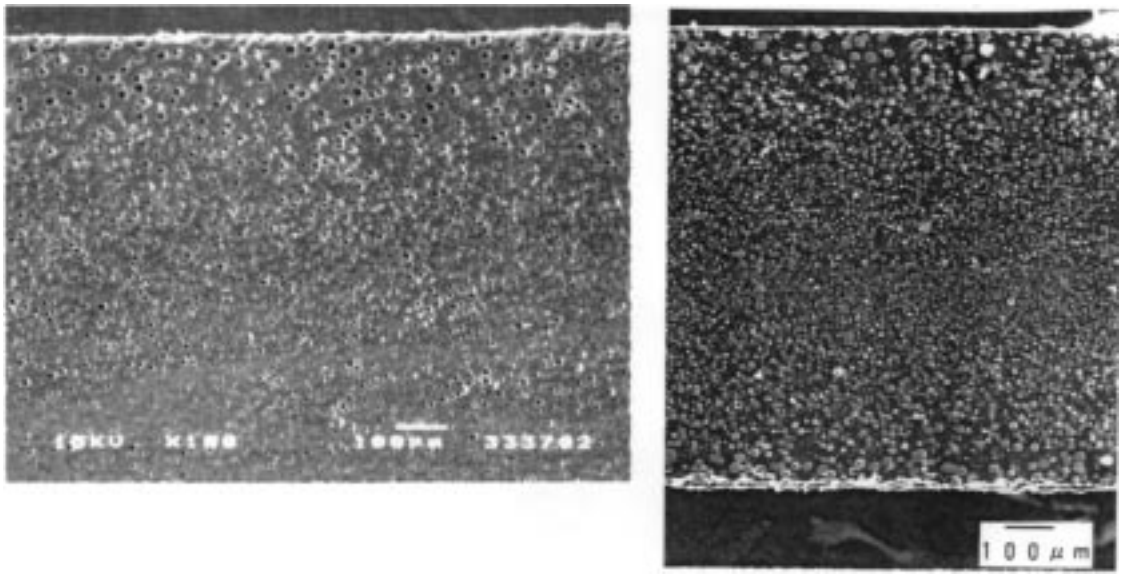

Figure 6. SEM micrographs of the cross section of the 70/30 PP/EVAc blends of 2 and 1 mm thicknesses annealed at 220 °C for 70 min.

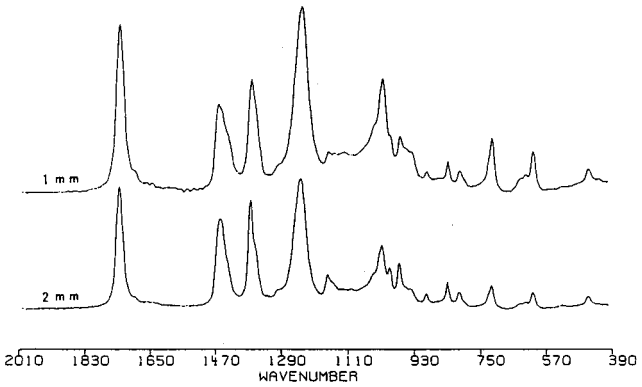

Figure 7. ATR-FTIR spectra on the surface of the 70/30 PP/EVAc blends with 1 and 2 mm thicknesses at 220 °C for various annealing times.

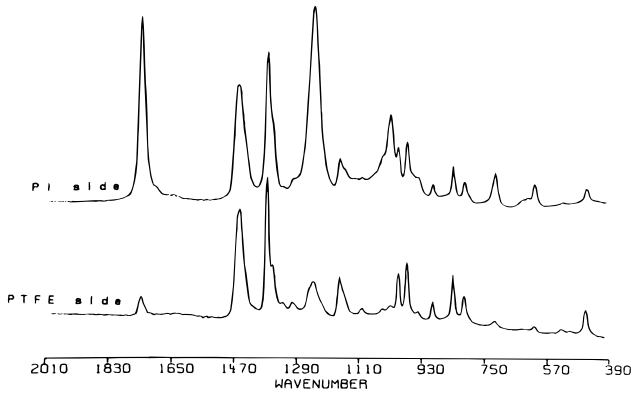

Figure 8. ATR-FTIR spectra of the two side surfaces of the 70/30 PP/EVAc blend sample laminated between the PI and PTFE films.

Figure 8 shows the spectra of the two side surfaces of the blend, i.e., the surfaces in contact with the PI and PTFE films in the annealing process. It is seen that the absorption intensity of the 1737 cm^{-1} band is much stronger for the sample surface contacted with PI than with PTFE. This means that the EVAc component preferentially accumulates on the blends/PI film interface, suggesting the minimization of the interfacial energy at the substrate/polymer blends interface. This result indicates that the accumulation of the dispersed phase on the surface can be accelerated by the formation of the gradient phase morphology in the blends, but the surface composition is greatly affected by the interfacial energy at the polymer/substrate interface.

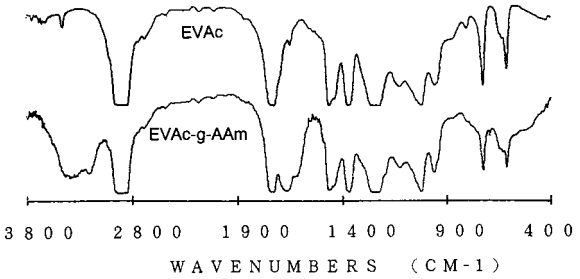

Figure 9. FTIR spectra of the EVAc and refined EVAc-*g*-AAm melt-grafted samples.

As already mentioned above, the longer the annealing time and the higher the annealing temperature, the more the particle size of the dispersed phase increased from the inside to the surface. With the formation of the gradient phase structure, the EVAc components accumulated on the surface of the polymer blends. This suggests that the surface composition of the polymer blends can be freely adjusted by controlling the gradient dispersed phase formation.

If some desired functional monomers can be grafted onto EVAc, with the grafted EVAc as a carrier, the grafted polar groups should be transported onto the surface of the material while forming an EVAc gradient dispersed phase in the PP/grafted EVAc blends. Thus, the goal of effective improvement of the material surface properties could be achieved.

In this work, the melt-grafting reaction of the AAm monomer on EVAc was carried out using a Brabender. The IR spectrum of the refined EVAc-*g*-AAm melt-grafted sample is shown in Figure 9. It was observed that the $-NH_2$ absorption bands appeared in the range 3500−3200 cm^{-1} in the EVAc-*g*-AAm spectrum. These results show that a portion of the AAm has been introduced into EVAc. The EVAc-*g*-AAm was then blended with PP. The relationship between the gradient dispersed phase formation and surface properties of the PP/EVAc-*g*-AAm blends is discussed.

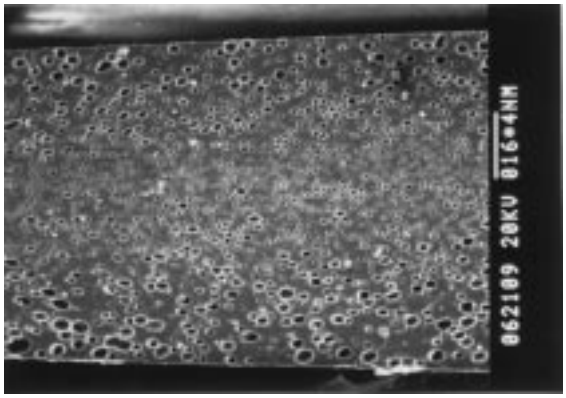

Figure 10. SEM micrograph of the cross section of the 70/30 PP/EVAc-*g*-AAm blends annealed at 220 °C for 70 min.

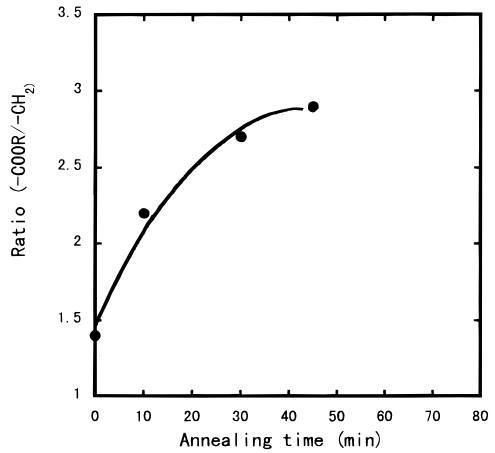

Figure 11. Plot of $-COOR/CH_2$ ratio in spectra of PP/EVAc-*g*-AAm blends annealed at 220 °C versus annealing times.

After annealing, the cross section of the phase structure of the EVAc-*g*-AAm and PP blend was observed with SEM. Figure 10 shows the SEM micrograph of the cross section of the 70/30 PP/EVAc-*g*-AAm blend annealed at 220 °C for 70 min. The gradient phase structure was also formed, similar to the PP/EVAc blend systems. As the temperature rises and time lengthens during the heat treatment, the gradient structure of the dispersed phase constantly develops. This result not only supports the universal gradient phenomenon of polymer blends but also provides a new way of modifying surface properties through molecular design and phase morphology control.

The results of the surface composition examination for the blends show that as the temperature rises and time lengthens during the heat treatment, i.e., with the development of the gradient dispersed phase, the dispersed phase component of the surface constantly increases. This means that the AAm grafted on the EVAc will come out on the surface of the blend in the form of the dispersed phase gradient to modify the polarity of the sample surface. Figure 11 illustrates the relationship between the intensity of the IR absorption bands of C═O of the grafted EVAc on the PP/EVAc-*g*-AAm blend surface and the annealing time. The longer the annealing time, the stronger the intensity of the bands. This shows that the component of the grafted EVAc on the blend surface will increase with increasing annealing time. The same result can be obtained by increasing the annealing temperature. This result means that the EVAc component accumulated on the surface of the blend with the formation of the gradient phase

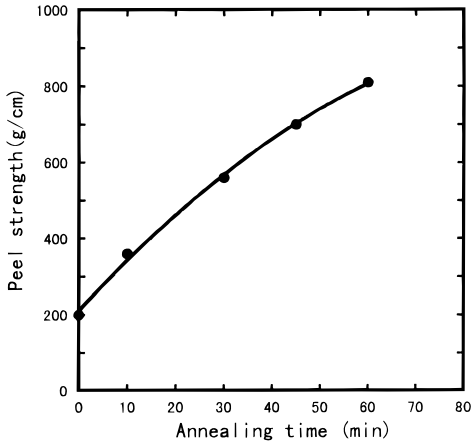

Figure 12. Peeling strength of the coating versus annealing times for the PP/EVAc-*g*-AAm blends.

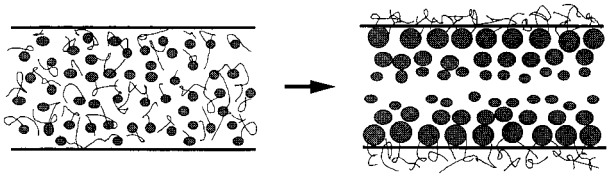

Figure 13. Schematic diagram of surface modification through formation of gradient phase morphology of polymer blends.

morphology. The AAm grafted on the EVAc should be brought to the sample surface with the EVAc.

To confirm the accumulation of the functional monomer AAm on the blend surface together with the dispersed phase EVAc, the PU paints were coated on the surface of the PP/EVAc-*g*-AAm blend samples at 80 °C without primer. After drying at 120 °C, the coating adhesion was tested. Figure 12 shows the changes in the peeling strength with increasing annealing times for the PP/EVAc-*g*-AAm blends. The peeling strength increases with increasing annealing time and reached 800 g/cm when the annealing time was 60 min. The tendency of the increasing peeling strength with the increase in annealing time is similar to that of the grafted EVAc on the sample surface of the blend as shown in Figure 11. This implies that since the dispersed phase with polar groups came out on the blend surface with increasing annealing time, the hydrogen-bonding interaction between the amine group, $-NH_2$, in the grafted EVAc and the isocyanate group, $-N-C-O$, in the PU paints should be formed. It also resulted in increases in the peeling strength of the coating with increasing annealing time.

The above results indicate a possible way to obtain materials with desired surface properties through molecular design and gradient phase morphology control. Figure 13 shows the scheme of surface modification through formation of a gradient morphology in the blends. Thus, with EVAc as a carrier, the grafted polar groups were transported onto the surface of the material while forming an EVAc gradient dispersed phase.

Conclusions

(1) The 70/30 blend of PP and EVAc blends formed a gradient phase morphology in the cross section by annealing. It was found that the EVAc component on the surface of the blends after annealing increased with increasing annealing time and temperature using ATR-FTIR and ESCA. This means that the EVAc component

accumulates on the surface with the formation of the gradient morphology in the blends. Also, the more the gradient phase morphology formed, the more the EVAc component enriched the sample surface.

(2) No significant difference in the gradient phase morphology was found for both the thin and thick PP/EVAc blend samples under the same annealing conditions. The accumulation of the dispersed phase component does not depend on the sample thickness but depends on the formation of the gradient phase morphology.

(3) The component accumulation on the surface of the blends was greatly influenced by what substrates the blend samples are in contact with during the annealing process, because of the minimization of the interfacial energy at the substrate/polymer blend interface. This result indicates that the accumulation of the dispersed phase on the surface can be accelerated by the formation of the gradient phase morphology in the blends, but the surface composition is significantly affected by the interfacial energy at the polymer/substrate interface.

(4) It was found that PP/EVAc-*g*-AAm formed the gradient phase structure during annealing, like the PP/EVAc blend system.

(5) The formation of the gradient phase structure resulted in the accumulation of the functional AAm groups on the sample surface. The hydrogen-bonding interaction between the paints and the functional groups grafted on the dispersed phase EVAc improved the coating adhesion, indicating that the gradient phase structure control of blends is an effective way for materials surface modification.

Acknowledgment. Prof. Xu-Ming Xie is indebted to the National Natural Science Foundation of China (Grant No. 29604004), to the Excellent Young Teacher Foundation of State Education Commission of China, and to the Research Fund of the China Petrochemical Corporation for their financial support.

References and Notes

(1) Thomas, H.; O'Malley, J. J. *Macromolecules* **1981**, *14*, 1316.
(2) Takahara, A.; Tashita, J.; Kajiyama, T.; Takayanagi, M.; Macknight, W. J. *Polymer* **1985**, *26*, 978.
(3) Chujo, R.; Nishi, T.; Sumi, Y.; Adachi, T.; Naito, H.; Frentzel, H. *J. Polym. Sci., Polym. Lett. Ed.* **1983**, *21*, 487.
(4) Cowie, J.; Devlin, B.; McEwen, I. *Polymer* **1993**, *34*, 501.
(5) Xie, X.-M.; Matsuoka, M.; Takemura, K. *Polymer* **1992**, *33*, 1996.
(6) Composto, R. J.; Stein, R. S.; Kramer, E. J.; Jones, R. A. L.; Mansour, A.; Karim, A.; Felcher, J. P. *Physica B* **1989**, *23*, 2584.
(7) Xie, X.-M.; Xiao, T.-J.; Zhang, Z.-M.; Tanioka, A. *J. Colloid Interface Sci.* **1998**, *206*, 189.
(8) Schroeder, K.; Klee, D.; Hocker, H.; Leute, A.; Benninghoven, A.; Mittermayer, C. *J. Appl. Polym. Sci.* **1995**, *58*, 699.
(9) Schmitt, R. L.; Gardella, J. A., Jr.; Magill, J. H.; Salvati, L., Jr.; Chin, R. L. *Macromolecules* **1985**, *18*, 2675.
(10) Anastasiadis, S. H.; Russel, T. P.; Satijaand, S. K.; Majkrzak, C. F. *J. Chem. Phys.* **1990**, *92*, 5677.
(11) Miki, T.; Kouzai, K.; Yonemura, U. *Polym. Prepr. Jpn.* **1990**, *38*, 1281.
(12) Grassley, W.; Krishnamoorti, R.; Balsara, N.; Fetter, L. J.; Lohse, D. J.; Sissano, J. A. *Macromolecules* **1993**, *26*, 1137.
(13) Frederickson, G.; Liu, A.; Bates, F. S. *Macromolecules* **1994**, *27*, 2503.
(14) Schaub, T. F.; Kellog, G. J.; Mayes, A. M.; Kulasekere, R.; Anker, J. F.; Kaiser, H. *Macromolecules* **1996**, *29*, 3982.
(15) Xie, X.-M.; Matsuoka, M.; Takemura, K. *Polym. Prepr. Jpn.* **1991**, *40*, 2800.
(16) Xie, X.-M.; Hu, W.; Chen, Y.; Tanioka, A. *Polym. Prepr. Jpn.* **1994**, *43*, 3842.
(17) Xiao, T.-J.; Xie, X.-M. IUPAC Symposium on Macromolecular Condensed State, Beijing, Aug 1996.
(18) Xie, X.-M.; Xiao, T.-J.; Yang, Y. *Chem. J. Chin. Univ.* **1998**, *11*, 1864.

MA9805046